Open Access

Max Schmiedel*, Anita Moeller, Martin A. Koch and Alfred Mertins

Designing a compact MRI motion phantom

DOI 10.1515/cdbme-2016-0104

Abstract: Even today, dealing with motion artifacts in magnetic resonance imaging (MRI) is a challenging task. Image corruption due to spontaneous body motion complicates diagnosis. In this work, an MRI phantom for rigid motion is presented. It is used to generate motion-corrupted data, which can serve for evaluation of blind motion compensation algorithms. In contrast to commercially available MRI motion phantoms, the presented setup works on small animal MRI systems. Furthermore, retrospective gating is performed on the data, which can be used as a reference for novel motion compensation approaches. The motion of the signal source can be reconstructed using motor trigger signals and be utilized as the ground truth for motion estimation. The proposed setup results in motion corrected images. Moreover, the importance of preprocessing the MRI raw data, e.g. phase-drift correction, is demonstrated. The gained knowledge can be used to design an MRI phantom for elastic motion.

Keywords: motion artifacts; motion phantom; MRI.

1 Introduction

Magnetic resonance imaging (MRI) is one of the most important imaging modalities in clinical routine today. Especially, the superior tissue contrast and the absence of ionizing radiation make MRI a vital tool for diagnosis. These upsides come with a longer time for image acquisition compared to computed tomography, which makes MRI particularly susceptible to motion artifacts [1]. In particular in thorax imaging, there is body motion due to respiration and cardiac motion. Breath holding is one way to avoid respiratory motion artifacts [2] but it is inconvenient and not suitable for all patients and imaging schemes. This and cardiac motion, which is inevitable, make it necessary to deal with the problem of motion artifacts on the level of data acquisition or data processing. A way to do so are prospective and retrospective gating. In both cases, additional information to the complex k-space data is needed.

It is desirable that motion corruption could be estimated just with the complex MRI raw data without additional measurements or trigger signals. One approach for such a blind motion compensation algorithm is presented in [3]. To test this blind motion compensation algorithm on real reproducible measurement data, a motion phantom needs to be utilized. Even though, there are commercially available MRI motion phantoms, none of them can be used in a small animal MRI system.

In this work, an MRI phantom for rigid motion is presented, which can be used in a small animal MRI system. Furthermore, results of motion corrupted imaging and retrospective gating are displayed.

2 Material and methods

For all experiments, an 1 T ICON TM MRI system (Bruker, Ettlingen, Germany) was used. It is designed for imaging small rodents and is based on a permanent magnet. The gradient system provides gradients up to 360–390 mT/m. All data were acquired with a mouse body transmit-receive coil.

2.1 Imaging sequence

For all images, data were acquired using a fast low angle shot sequence (FLASH) [4]. For a good signal-to-noise ratio (SNR) a strong signal with a high echo amplitude is needed. The echo amplitude for basic gradient echo sequences like FLASH can be described as

$$A_E = M_z^0 \frac{1 - e^{-T_R/T_1}}{1 - \cos(\alpha) \cdot e^{-T_R/T_1}} \sin(\alpha) e^{-T_E/T_2^*} \qquad (1)$$

with $M_z{}^0$ the longitudinal magnetization in thermal equilibrium, T_R the repetition time, T_E the echo time, α the

***Corresponding author: Max Schmiedel,** Medical Engineering Science, Ratzeburger Allee 160 23562 Lübeck, Germany, E-mail: max.schmiedel@student.uni-luebeck.de
Anita Moeller and Alfred Mertins: Institute for Signal Processing, Ratzeburger Allee 160 23562 Lübeck, Germany, E-mail: moeller@isip.uni-luebeck.de (A. Moeller), E-mail: mertins@isip.uni-luebeck.de (A. Mertins)
Martin A. Koch: Institute of Medical Engineering, Ratzeburger Allee 160 23562 Lübeck, Germany, E-mail: koch@imt.uni-luebeck.de

flip angle, T_1 the longitudinal relaxation time, and $T_2^\star$ the transverse relaxation time as shown in [5].

In this work, repetition times of 50 ms, echo times of 6 ms and flip angles of 15° were used.

The direction of object motion was chosen as phase-encoding direction. For periodic motion, this may cause motion artifacts if

$$T_{acq} > \frac{1}{2mf_0} \tag{2}$$

with T_{acq} the acquisition time for all phase-encoding steps, the mth harmonic of the periodic movement and f_0 the frequency of the object motion [5]. For the first harmonic and the chosen 0.43 Hz motion frequency, (2) limits the acquisition time to 1.16 s if motion artifacts are to be avoided. With 3.2 s the acquisition time was chosen in a way that motion artifacts will appear.

2.2 Phase drift correction

In case of retrospective gating, one has to deal with longer times for imaging, since multiple repetitions are needed. For this work, a data acquisition time of 10 min for 200 repetitions was needed. In these dimensions, phase-drifts become relevant. Over time the total transverse magnetization drifts in phase but stays constant in magnitude for the same time after excitation. The oscillating signal here in complex notation can be described as

$$S(t) = S_0 \cdot e^{i(\omega_{rf} t + \phi(t))} \tag{3}$$

with S_0 being the magnitude of the signal, ω_{rf} the precession frequency and $\phi(t)$ the initial phase. For short imaging times, $\phi(t)$ can be assumed as constant. However, over longer times, $\phi(t)$ is not constant and results in a translation in image space. For combining data which is spread over several minutes in time, as needed for retrospective gating, a phase correction has to be performed as a phase subtraction so that

$$\phi_{in} = \phi_{ac}(t) - \phi_{co}(t) \tag{4}$$

with ϕ_{in} the phase for the initial repetition, $\phi_{ac}(t)$ the actual phase for a chosen repetition, and $\phi_{co}(t)$ the phase-correction value. Therefore, the sampled data was corrected by multiplication with a time dependent term

$$e^{i(-\phi_{co}(t))}. \tag{5}$$

The repetition-dependent $\phi_{co}(t)$ is determined by fitting the phase for all phase-encoding steps with the same number and the same motor position with a 4th degree polynomial (see Figure 1).

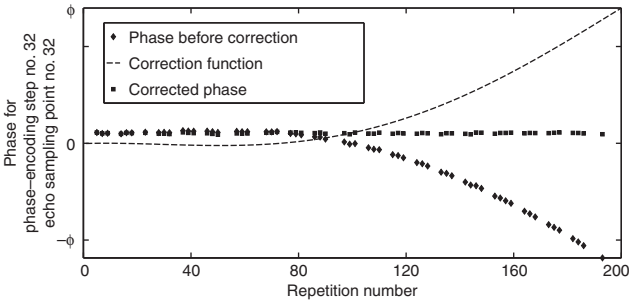

Figure 1: Phase for diffrent repetitions with the same corresponding motor position, phase-encoding step and echo sampling point.

If the phase-drift remains uncorrected, wave-like artifacts appear due to not corresponding phase values of the combined data of different repetitions. This effect is shown subsequently in the results section.

2.3 Motion phantom

The motion phantom is designed in a way that rigid object motion can be imaged with an MRI system.

It consists of an inner part, placed inside the MRI system, and an outer part, placed right next to the MRI system. The outer part consist of an electro motor RE50 (maxon motor GmbH, München, Germany) and a translation stage. It is used to generate a force to deform the inner part of the phantom. Both parts are connected via a polyethylene line. The electro motor rotates periodically and the rotation is transformed to a linear movement by a translation stage. This movement is transferred to the inner phantom part via the line and causes a translational relative movement between a small diameter test tube (length/inner diameter/outer diameter: 100/20/22 mm) and a fixed large diameter test tube (90/13/18 mm). To reverse the translation of the inner phantom part, an elastic band is used. The imaged object, an agarose cylinder, is placed in the small diameter test tube. A schematic overview of the phantom is shown in Figure 2. The agarose has a concentration of 0.75% and is prepared under laboratory conditions. Therefor, agarose powder (Natura, Hannover, Germany) was boiled in pure water for five minutes.

2.4 Triggering for retrospective gating

For retrospective gating, trigger signals of the phantom and the MRI system are needed to assign the measured data to the corresponding phantom motion status. The trigger signals are rectangular voltage changes and denoted as pulses in the following.

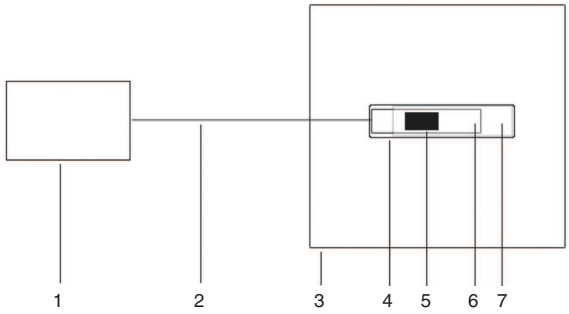

Figure 2: Overview of the motion phantom: (1) translation stage/motor, (2) line, (3) MRI system, (4) elastic band, (5) agarose cylinder, (6) moved test tube, (7) fixed test tube.

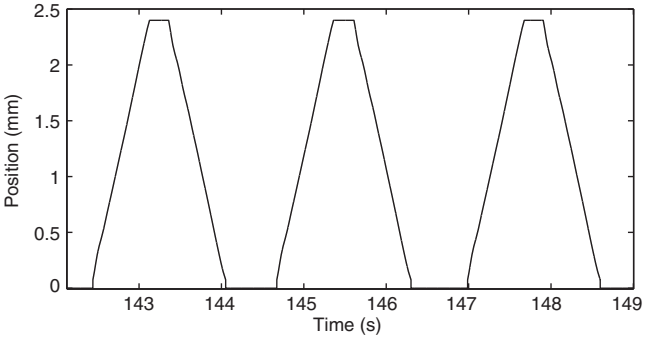

Figure 3: Section of the assumed movement of the translation stage. The movement between two trigger signals was approximated as linear.

The motor control sends a trigger signal with a pulse width of 100 µs every 13.5° of motor rotation which corresponds to a linear movement of the motion phantom of 75 ms. With these pulses the motion of the phantom can be approximated. Therefore, the movement between two trigger signals is assumed to be linear. The result is shown in Figure 3.

The MRI system sends a trigger signal with a pulse width of 1 ms before every phase-coding step. The time for frequency coding is approximated as two times the echo time. With the used motor rotation speed of 100 rpm and an echo time of 6 ms this results in an object motion of 10 µm during frequency coding. Compared to a voxel size of 781 µm in the direction of movement, the motion during frequency encoding is considered negligible.

2.5 Image reconstruction and retrospective gating

During data acquisition, the k-space is fully Cartesian-sampled but the contained data is phase-drift- and motion-corrupted. Therefore, the phase-drift correction has to be carried out prior to reconstruction.

To show the influence of object motion on the reconstructed images, a 2D inverse fast Fourier transform is applied to the k-space data. In case of the retrospectively gated images, before applying a 2D inverse fast Fourier transform, data binning was executed as follows.

The motor position was discretized in intervals with an interval width of 0.2 mm. With a total moving distance of 2.5 mm this makes 13 bins for the gating process. Now the data for individual k-space lines are sorted into bins according to the motor position at the time of their echo middle. All bins contain data for all rows of k-space. The difference between data of different repetitions of a specified phase-encoding step in one bin can be considered negligible, so the repetition to be used can be chosen randomly within one bin.

3 Results and discussion

As it can be seen in Figure 4A, image reconstruction for an static agarose cylinder was performed successfully. With the chosen imaging parameters, an SNR of 32 could be achieved. It was calculated manually by the ratio of the means of object and background values.

In Figure 4B, an image of the first repetition which was corrupted due to rigid object motion can be seen. The mean square error (MSE) between the motion-corrupted image and the image without motion amounts to 140. Compared to a mean signal value in the region of interest of 150, the MSE indicates artifacts in the motion-corrupted image. Visual examination reveals noticeable artifacts in the direction of motion. The object appears to be shortened in the motion-corrupted image.

3.1 Gating

The results of the gating process can be seen in Figure 4D–F. The movement was split in 13 bins for gating and the positions 0 mm, 1 mm and 2 mm were chosen for visualization. The position 0 mm corresponds to a pause in the periodic movement which can be seen in Figure 3. Therefore, the MSE between the gated image (pos. 0 mm) and the image with no object motion should be zero for a perfect gating process. In fact the MSE amounts to 39. Visually, there can not be identified much difference. The reason for that is a difference in the mean values in the region of interest. That is caused by the not entirely perfect equilibrium state of the longitudinal magnetization. The motionless image was acquired within one repetition, whereas the gated image consists of the first seven repetitions. An

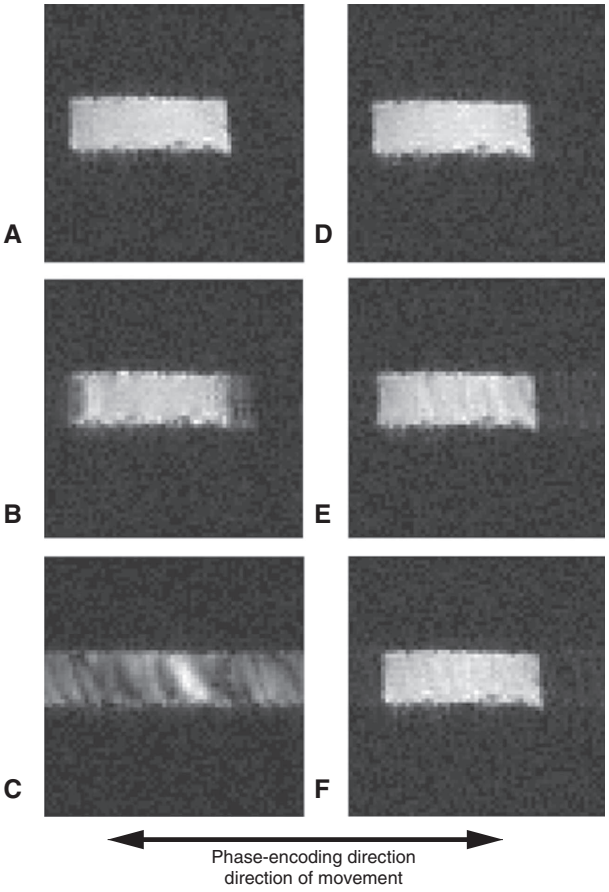

Figure 4: Images (64 × 64) of the agarose cylinder: (A) no motion (B) periodical movement (C) gated with periodical movement and without phase correction (D) gated with periodical movement and phase correction (pos. 0 mm) (E) gated with periodical movement and phase correction (pos. 1 mm) (F) gated with periodical movement and phase correction (pos. 2 mm).

observation of the raw data revealed that the signal at the beginning of a data acquisition is slightly higher than in the following repetitions.

For perfect gating, the image at position 1 mm should be a shifted version of Figure 4A and Figure 4D. Because of that, the image (pos. 1 mm) was manipulated applying a shift in the opposite direction and than the MSE to the image with no motion was calculated. The result is an MSE of 62. The fact of the small error reveals that a correction has been performed, but it seems as it has been less successful than in the case for the position 0 mm. This is probably caused by the phase-drift. A phase-drift correction was performed, which had a big impact that can be recognized by comparing Figure 4D–F with Figure Figure 4C. Nevertheless, experiments with the data that is chosen for the gating process revealed that the gating result becomes better if the chosen data belongs to successive repetitions (data not shown).

For the gated image at position 2 mm, the results are similar to the position 1 mm.

3.2 Motion phantom

Analysis of the gated images revealed that there was an object motion of about 3 pixels. With a voxel width in the direction of movement of 0.78 mm this corresponds to 2.3 mm of object motion. Therefore, it can be assumed that almost the full movement of the translation stage could be transferred to the inner phantom. This validates the chosen phantom design.

4 Conclusion

In this work, a compact and easy to use phantom for rigid object motion was designed. It was shown that retrospective gating based on motor trigger signals can be performed. The object movement was reconstructed and can be used as the ground truth for motion estimation. The preprocessing of the raw data, e.g. phase-drift correction, was carried out succesfully. In further examinations, the gating process as implemented needs to be examined with elastic motion and therefore the motion phantom has to be modified. If successful, the data can be used as reference for blind motion compensation algorithms as presented in [3].

Author's Statement
Research funding: The author state no funding involved. Conflict of interest: Authors state no conflict of interest. Material and Methods: Informed consent: Informed consent has been obtained from all individuals included in this study. Ethical approval: The conducted research is not related to either human or animal use.

References

[1] Tavallaei MA, Johnson PM, Liu J, Drangova M. Design and evaluation of an MRI-compatible linear motion stage. Med Phys. 2016;43:62–71.
[2] Zaitsev M, Mclaren P, Herbst M. Motion artifacts in MRI: a complex problem with many partial solutions. J Magn Reson Imaging 2015;42:887–901.
[3] Möller A, Maaß M, Mertins A. Blind sparse motion MRI with linear subpixel interpolation. Bildverarbeitung für die Medizin. 2015:510–5.
[4] Nitz WR, Runge VR, Schmeets SH, Faulkner W, Desai NK. Praxiskurs MRT. 1st ed. Stuttgart: Georg Thieme Verlag KG 2007.
[5] Liang ZP, Lauterbur PC. Principles of magnetic resonance imaging. 1st ed. New York: IEEE Press; 2000.